

Article

Genesis and Distribution of Low Fluvial Terraces Formed by Holocene Climate Pulses in Brazil

Archimedes Perez Filho ¹, Vinícius B. Moreira ² , Luca Lämmle ^{1,*} , André O. Souza ³ , Bruno A. Torres ¹ , Pedro I. C. Aderaldo ¹, Éverton V. Valezio ¹ , David O. B. F. Machado ¹, Mateus M. Prebianca ¹ , Alysson F. Mazoni ¹, Carolina Zabini ¹  and Felipe G. Rubira ⁴ 

¹ Institute of Geosciences, University of Campinas (UNICAMP), Campinas 3083-855, Brazil

² Institute of Geosciences and Exact Sciences, São Paulo State University (UNESP), Rio Claro 13506-900, Brazil

³ Center for the Humanities, Federal University of Western Bahia (UFOB), Barreiras 47805-100, Brazil

⁴ Institute of Natural Sciences, Federal University of Alfenas (UNIFAL-MG), Alfenas 3701-9000, Brazil

* Correspondence: lucalammle@ige.unicamp.br

Abstract: Low fluvial terraces present azonal spatialization, encompassing several geomorphological compartments and climate zones in Brazil. Their genesis is directly related to river dynamics. When influenced by allogenic forces, such as Holocene climate pulses, it results in channel incision and posterior abandonment of the floodplain. Relatively plain landforms at different altimetric levels identified between the current floodplain and hillslope (low river terraces) are a result of these processes. Previous works using Optically Stimulated Luminescence (OSL) in low terraces of several rivers in Brazil have indicated morpho-chronologic similarities between depositional events, raising the hypothesis of feedbacks and fluvial adjustments relatively simultaneous to Holocene climate events. Considering these dynamics, this study employed OSL to obtain absolute dating information for 114 samples taken from distinct levels of the low river terraces of 30 rivers in Brazil, integrating the database of the IG-UNICAMP laboratory of Geomorphology and Environmental Analysis. Based on the data and statistical analysis (cluster and correlation analysis), this study aimed to identify relationships between different variables which might have controlled spatial homogenous and heterogeneous feedbacks during distinct paleoenvironmental contexts. The proposed methodology tested a fundamental hypothesis of the regional climatic geomorphology, and the results obtained may contribute to future discussions on the relationship between low river terraces and anthropic occupation.

Keywords: Brazilian rivers; spatial analysis; climatic geomorphology; OSL dating



Citation: Perez Filho, A.; Moreira, V.B.; Lämmle, L.; Souza, A.O.; Torres, B.A.; Aderaldo, P.I.C.; Valezio, É.V.; Machado, D.O.B.F.; Prebianca, M.M.; Mazoni, A.F.; et al. Genesis and Distribution of Low Fluvial Terraces Formed by Holocene Climate Pulses in Brazil. *Water* **2022**, *14*, 2977. <https://doi.org/10.3390/w14192977>

Academic Editor: Salvatore Ivo Giano

Received: 10 July 2022

Accepted: 19 September 2022

Published: 22 September 2022

Publisher's Note: MDPI stays neutral with regard to jurisdictional claims in published maps and institutional affiliations.



Copyright: © 2022 by the authors. Licensee MDPI, Basel, Switzerland. This article is an open access article distributed under the terms and conditions of the Creative Commons Attribution (CC BY) license (<https://creativecommons.org/licenses/by/4.0/>).

1. Introduction

Riverscapes are sets of natural components whose shapes result from complex and non-linear interactions among different processes, thresholds, and (pseudo) equilibrium [1–5]. Consequently, the response of river systems depends upon their emerging properties, the degrees of sensitivity to different allogenic inputs, and the connectivity between the different elements in the system [6–12]. From this perspective, the inherent complexity of river systems results in heterogeneous and nonlinear responses across time and space [7,13,14]. On the other hand, the internal evolution of the drainage basin is also an important issue, since the responses to allogenic inputs would be incorporated immediately, late, or may not even be influential on internal reorganizations [15–19].

Considering the complex relationship between paleoclimates and fluvial dynamics [6,20–26], the climate influences on river channels can be direct (such as variations in precipitation rates), indirect, and partial (vegetation). However, these complex responses concerning Tropical Rivers (TR) and Holocene Climate Pulses (HCP), are still largely unexplored and contrast with the greater progress in studies focusing on the complexities in

large river systems (Basin area > 10⁶ km²) [27–31]. In addition, climate inputs can generate different responses that depend on the attributes and spatial dimensions of the river system, indicating that smaller rivers hold important continental records on the Holocene paleoclimate events due to their greater sensitivity to subtle disturbances [11,20,32–44].

Currently, the Holocene is subdivided into the Meghalayan (Late Holocene –4250 years BP), Northgrippian (Middle Holocene, in the range of 8236–4250 years BP), and Greenlandian (Early Holocene, in the range of 11,700–8236 years BP) [45] Ages. These intervals are associated with environmental dynamics triggered by high-frequency and low-magnitude climate events, which mainly increased from the Middle Holocene [3,31,46–49]. For some authors, these dynamics were named Climate Pulses, and they induced adjustments in different riverscapes [26,28,36,38,39,50–54].

Previous studies have shown that the Roman Warm Period (300–1 CE), Dark Ages Cold Period (800–300 CE), Medieval Climate Anomaly (1300–800 CE), and Little Ice Age (1900–1300 CE) [16,46,55] were associated with oscillations in orbital dynamics, the release of sulfates during volcanic eruptions, an increase in CO₂ concentrations in the atmosphere, and a displacement of the Intertropical Convergence Zone (ITCZ) [15,46,56]. Furthermore, the colder–warmer climate oscillations presented environmental anti-phases between the Northern and Southern Hemispheres during the Late Holocene. Therefore, studies have shown different environmental conditions in humidity and temperature in the Southern Hemisphere [57–62].

Based on this, the low river terraces are landforms supported by alluvial deposits linked to abandoned floodplains [63,64] which record responses to short-term and low intensities climate and tectonic events [65]. These landforms differ from the floodplains as they are at higher altimetric levels and are formed by lateral and vertical erosion [50]. For this study, we considered the low terraces from a morpho-chronological perspective, so that the high and medium terraces are older than the low terraces analyzed. Nonetheless, these landforms are important records of human occupation [6,10,32,64–68] and also play an important ecological role to the development of biodiversity due to sediments and organic matter storage. However, these landforms have suffered considerable environmental stress, mainly from the 1970s onwards. Consequently, understanding the processes and dynamics associated with the low river terraces is useful for environmental management when the necessary mitigation of the negative impacts relating to the predicted climate dynamics over the next centuries are considered.

This study aimed to quali-quantitatively correlate the absolute ages of surficial cover at different levels of low river terraces from different regions of Brazil with Holocene Climate Pulses, by considering that low river terraces associated with small and medium-length rivers represent key elements relating to the climate factor acting on the dynamic adjustments of fluvial channels. Following the azonal spatialization of low river terraces, similar morphogenetic relationships with Holocene climate pulses were identified in different Brazilian environmental contexts. Therefore, this study is the first to analyze the morpho-dynamic and geochronology responses of a large number of small and medium-length rivers to short-term climate events, launching insights into the landscape evolution during the Holocene.

2. Materials and Methods

2.1. Selection and Spatialization of Geochronological Data

In total, the absolute dating of 114 Optically Stimulated Luminescence (OSL) surface cover samples associated with low river terraces were employed in the present study. In detail, all data collected from 30 rivers were obtained by the Environmental Analysis and Territorial Dynamics of the Laboratory of Geomorphology and Environmental Analysis IG-UNICAMP [27,34,36,37,41,42,44,66–73].

As shown in Figure 1, these river terraces were in different continental geomorphological macro-compartments and along the Brazilian coast (Supplementary Materials).

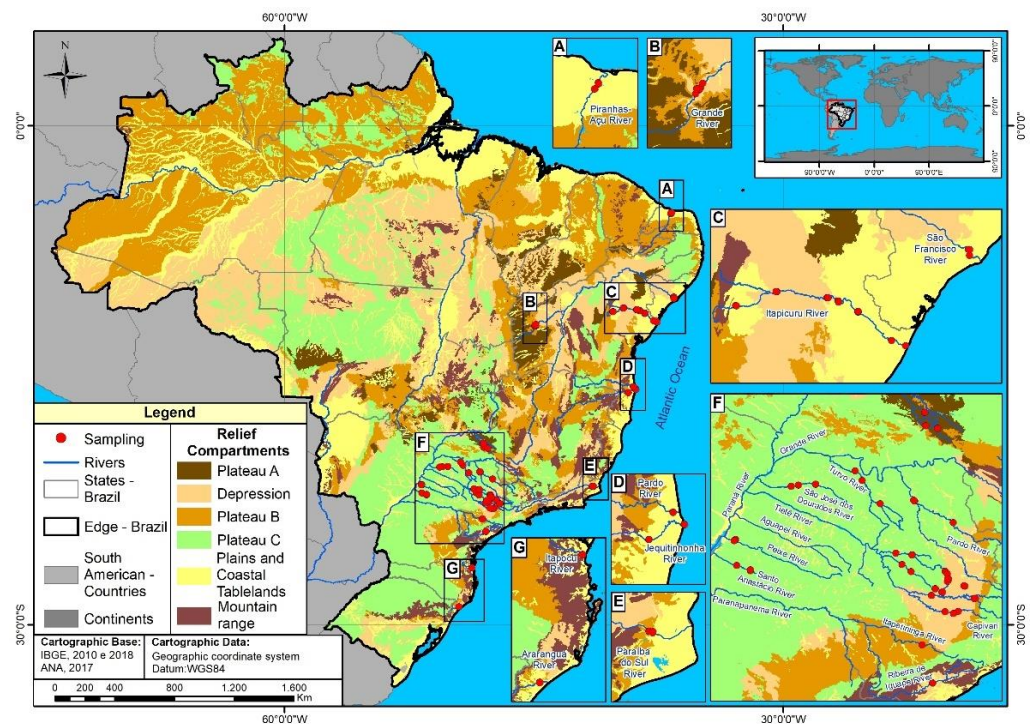


Figure 1. Location of sampling sites. (A) Low river terraces in the Piranhas-Açu river, Rio Grande do Norte state. (B) Low river terraces in the Grande river, Bahia state. (C) Low river terraces in the São Francisco river, Sergipe and Alagoas states, and the Itapicuru River, Bahia state. (D) Low river terraces in the Itapicuru, Una, Pardo, and Jequitinhonha rivers, Bahia state. (E) Low river terraces in the Paraíba do Sul river, Rio de Janeiro state. (F) Low river terraces in different rivers in the state of São Paulo. (G) Low river terraces in the Araranguá and Itapocu rivers, Santa Catarina state.

Within the scope of the continental morphological compartments of Northeast Brazil, absolute ages correspond to surficial covers associated with low terraces located at the middle course of the Itapicuru (see box C of Figure 1) [42,69,72] and Grande (see box B) rivers, both in the Southern Sertaneja Depression. Meanwhile, the areas analyzed in Southeast Brazil are associated with the Paulista Peripheral Depression [27,34,37], the Paulista Western Plateau [34,68], and the Uberlândia-Uberaba plateau on the edge of the Brazilian Central Plateau [70].

The morphological compartments located on the northeast coast correspond to the coastal lowlands and coastal plains in the mouths of the Piranhas (see box A), São Francisco (see box C), Jequitinhonha (see box D) [67,71], Itapicuru (see box C) [69], Una and Pardo (see box D) [74] rivers. Southeast coast areas are linked to estuaries and deltaic plains connected to the mouths of the Paraíba do Sul (see box E) and Ribeira do Iguape (see box F) [75] rivers. Regarding the southern coast of Brazil, we used data from the surficial covers of low terraces located on coastal plains associated with the mouth of the Araranguá (see box G) [36,76] and Itapocu (see box G) [73] rivers.

2.2. Identification of Low River Terraces

Low river terraces were identified through the analysis of geological and geomorphological cartographic databases and aerial photographs. We also employed radar images from the SRTM mission with a spatial resolution of 30 m (1 arc-second), and ALOS PALSAR (FBS) with a spatial resolution of 30 m (resampled to 12.5 m), obtained from the data portals of the USGS Earth Explorer (available online <https://earthexplorer.usgs.gov>) [accessed on 18 September 2022] and Alaska Satellite Facility (available online <https://asf.alaska.edu/>) [accessed on 18 September 2022], respectively. Compositions of high-resolution orbital

images available in the World Imagery plugin inherent to the QGIS Geographic Information System freeware software were also employed in terms of land/water humidity standards.

Topographic profiles were prepared based on transects transverse to the river courses through Digital Elevation Models (DEM). Fieldwork then confirmed the differentiation of the various levels through topography and pedological/sedimentary aspects. Radar images also contributed to the morphological characterization of surfaces when considering texture patterns, density, altimetry, structures, and the manipulation of color palette to distinguish surfaces which alternated between low amplitudes.

2.3. Optically Stimulated Luminescence (OSL)

The DATAÇÃO Laboratory (Datação, Comércio & Prestação de Serviços LTDA—São Paulo/SP, Brazil) performed the procedures using the SAR (Single Aliquot Regenerative-dose) method in quartz grains, as proposed by Wintle and Murray [77], with at least 15 aliquots (calibration curves) to determine the moment of deposition of the surficial cover in low river terraces.

Luminescence measurements were performed using grains (~10 to 30 mg) of a single sample repeatedly. Therefore, the accumulated dose of a sample was determined by the accumulated doses of several aliquots (histograms of equivalent doses and radial plot estimates), to verify that the luminescence signal was zero in the quartz grains [78]. This method decreased measurement error, making the ages obtained from the relationship between paleodose and annual dose values more statistically reliable.

The collection was carried out on surface covers which were composed of low river terrace levels, through the opening of trenches or exposed vertical profiles. As shown in Figure 2, PVC 60 cm × 6 cm pipes were introduced horizontally into the profiles so that the samples were not subjected to any kind of radiation. The edges were sealed, and the pipes were carefully removed after checking for complete filling and wrapped in black plastic bags.



Figure 2. Example of sample collection procedure for OSL dating. (A) Horizontal introduction of the PVC pipe at a certain depth of interest after opening the trench; (B) Pipes inserted and capped, ready to be taken out of the trench; (C) Pipes sealed in the laboratory ready to be sent for dating by OSL. (Photo by: L. Lämmle, April/2021).

Collection depths were defined based on the characteristics of the materials, peculiarities of the depositional layers, and pedological horizons. In addition, field adversities, such as the outcrop of subsurface waters, also limited deeper collections.

2.4. Data Processing and Statistical Correlations

An experimental table presented the variables which were converted to numbers or categories, whenever necessary, using Python modules. This meant that levels, regarded as words, were taken as sequential numbers 1, 2 and 3. Thus, the variables were altitude, age, longitude and level. As is common procedure for statistics and data analysis, the variables were normalized. This meant that the data were scaled using normal distribution as a scaler. This procedure highlights the variations between variables, so correlations are made clearer. In more detail, the Python module Sklearn was used for these steps, and graphs were plotted using Matplotlib and Seaborn tools.

3. Results

3.1. Geomorphic Characterization of Low Terraces

The results showed morphological patterns in the spatialization of low river terraces. The rivers presented up to three distinct levels, distributed in a paired and unpaired way along the riverbanks.

As illustrated in Figure 3, the terraces rise in the river valley at levels ranging from 1 to 20 m above the current river channel, and are always confined by the slopes that delimit the topography of these river forms [34]. It is important to highlight that the number of levels, distance, and elevation in relation to the river channel varies, since it depends on local environmental characteristics and the intensity of exogenous processes absorbed by the river system.

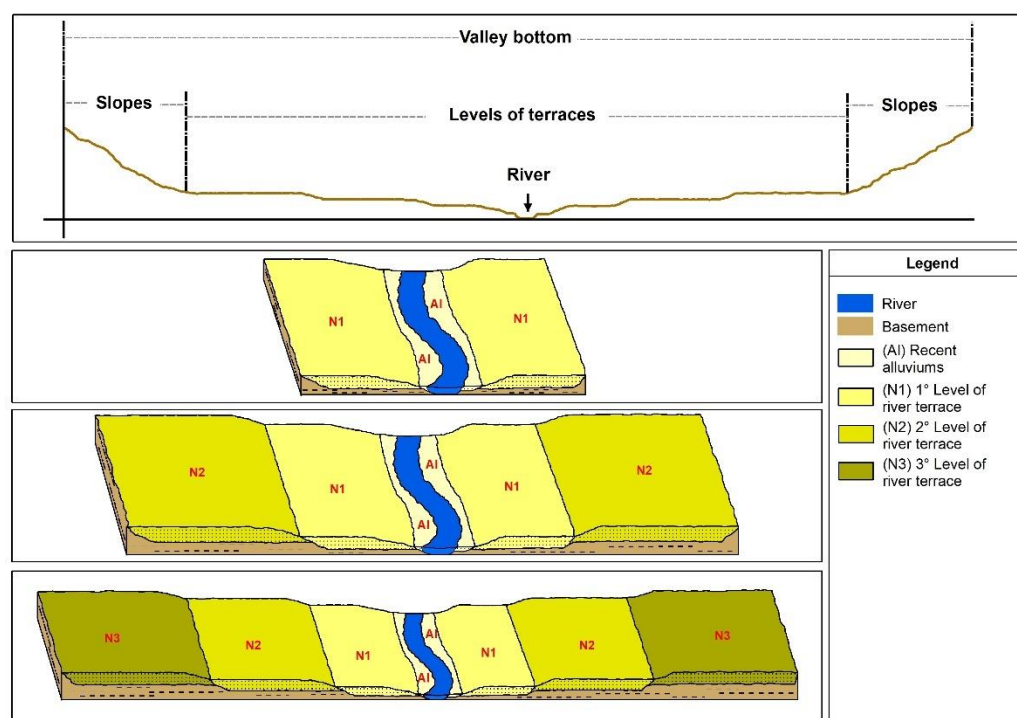


Figure 3. Schematic model of the distribution of low river terraces considered in the present study.

3.2. Statistical Data Analysis

The statistical analysis of data revealed clusters among the geochronological data. The medians of ages for the surficial covers indicated that the low terraces located in coastal geomorphological compartments are more recent than those of the inland continental compartments ($Md = 0.585$ and $Md = 1.325$, respectively).

As shown in Figure 4, there is a predominance of Level 1 low terraces compared to levels 2 and 3, and in many cases, there was only a single level. This suggested that most rivers in the compartment had a vertical incidence only once during the Late Holocene, unlike

rivers located in the inland continental compartments, which showed mostly staggering levels.

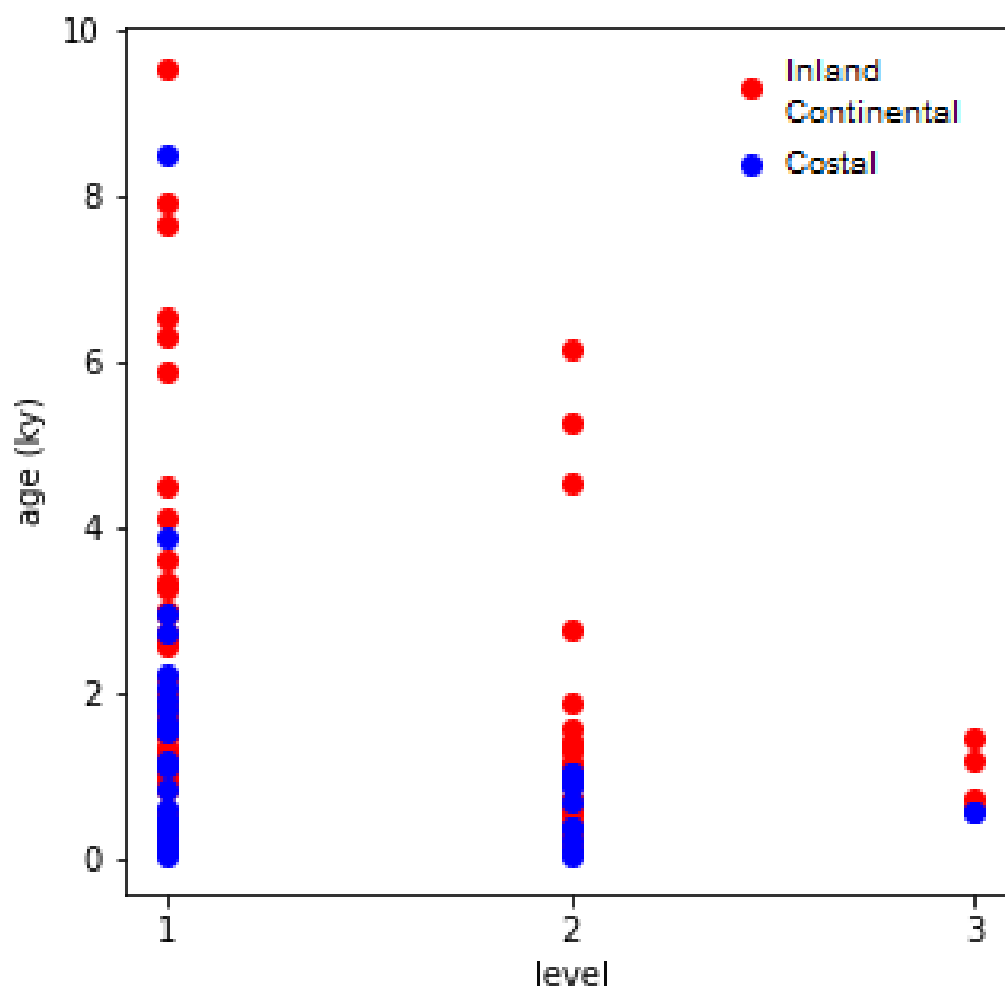


Figure 4. Age distribution of samples and their terrace levels. Each dot represents a sample with its age and terrace level (1, 2, and 3). Coastal samples are younger and present a smaller age distribution than continental samples.

Considering the variance by geomorphological subcompartment and low terrace levels, the inland subcompartments of the São Francisco Craton and the Paulista Western Plateaus showed older ages, with mean values of 5234 ka and 6713 ka, respectively.

By analyzing the same subcompartments in the boxplots presented in Figure 5, it was possible to observe the variation in the concentration of ages, demonstrating the distinctive behavior under the area of occurrence and environmental conditions.

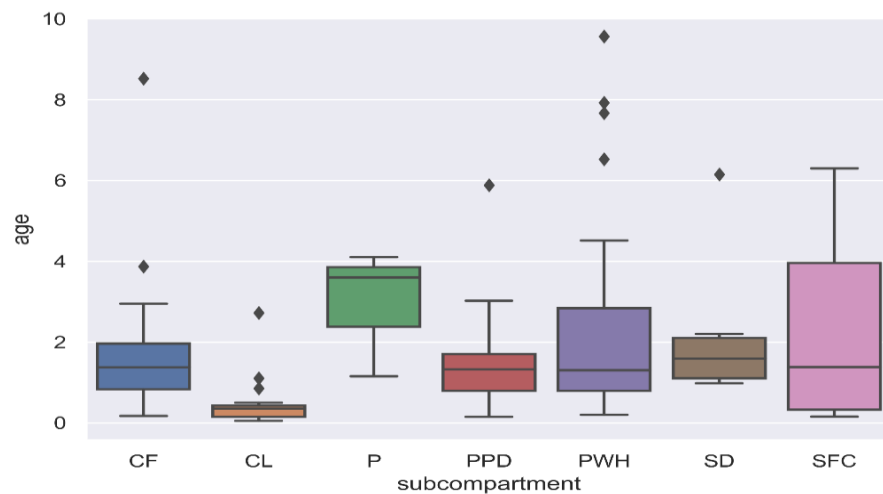


Figure 5. Subcompartment boxplot of the ages of the samples; CP: Coastal Plains; CL: Coastal Lowland; P: Plateau; PPD: Paulista Peripheral Depression; PWP: Paulista Western Plateau; SD: Sertaneja Depression; SFC: São Francisco Craton.

Regarding the correlation matrix shown in Figure 6A, a greater correlation was detected between latitude and longitude, and between compartments and subcompartments, to the detriment of the other variables. The values obtained were close to 1.0, indicating a significant degree of positive correlation. These results are reinforced by the two following Principal Components Analysis (PCA) results represented in Figure 6B,C, where it is possible to see that the explained variance from the two illustrated components equates to 64.69% of the total variance. Also, in Figure 6B,C, the best groupings of spatial distribution variables were observed between the inland/coastal continental compartments and subcompartments, suggesting morphogenetic distinctions between the inland and coastal groups, as well as the inland subgroups.

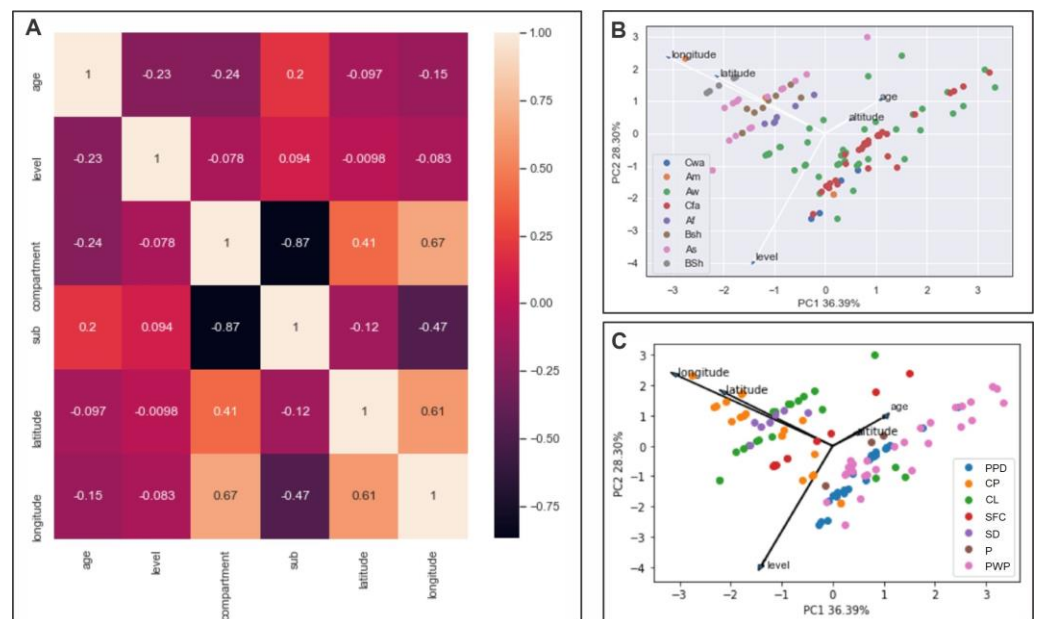


Figure 6. (A) Correlation matrix: the image shows the correlations between variables. Correlations are calculated using normalized values. (B) Principal Component Analysis (PCA) between continental compartments based on the Köppen climate classification, and (C) between geomorphological subcompartments, respectively.

The two main components contain 64.69% (36.39% + 28.30%) of the data variation, which means that data variation is almost 65%, and is summarized by the two main components. Latitude and longitude present similarly in sample variation (Figure 6B,C). They are also unrelated to age and altitude, nearly orthogonal (Figure 6B,C). Age and altitude are also closely related to each other, and terrace level is strongly related to age and altitude (in the opposite direction) and weakly related the geographic position (latitude and longitude). Climate subcompartments can be mostly distinguished, along with geographic coordinates (Figure 6B,C).

4. Discussion

4.1. Paulista Peripheral Depression, Paulista Western Plateau, and Central Plateau

The results presented in Figure 7a,b indicated a concentration of depositional ages synchronous to the cooling pulses of the northern hemisphere [15,54] and humid conditions related to the increase in precipitation inherent to sudden variations in the South American Monsoon System (SAMS) [79,80]. In detail, yellow dots correspond to the samples from the Brazilian Central Plateau [70]. Brown dots correspond to samples from the Paulista Western Plateau [34,68]. Orange dots correspond to samples from the Paulista Peripheral Depression [7,37,68]. Horizontal bars indicate the standard deviation of dating. Vertical gray bars indicate Bond events from 0 to 6 [15,56], adapted from Strikis et al. [79], Cheng et al. [80], and Zielhofer et al. [81]. The deposition of materials from low river terraces located in Southeastern Brazil occurred during rainy events, and correlated with Bond events centered at 9.4/8.2/7.5/5.9/4.2/2.7/1.6/0.4 ka [54,79–81]. Such dynamics possibly led to more frequent flood pulses in the rivers assessed [41].

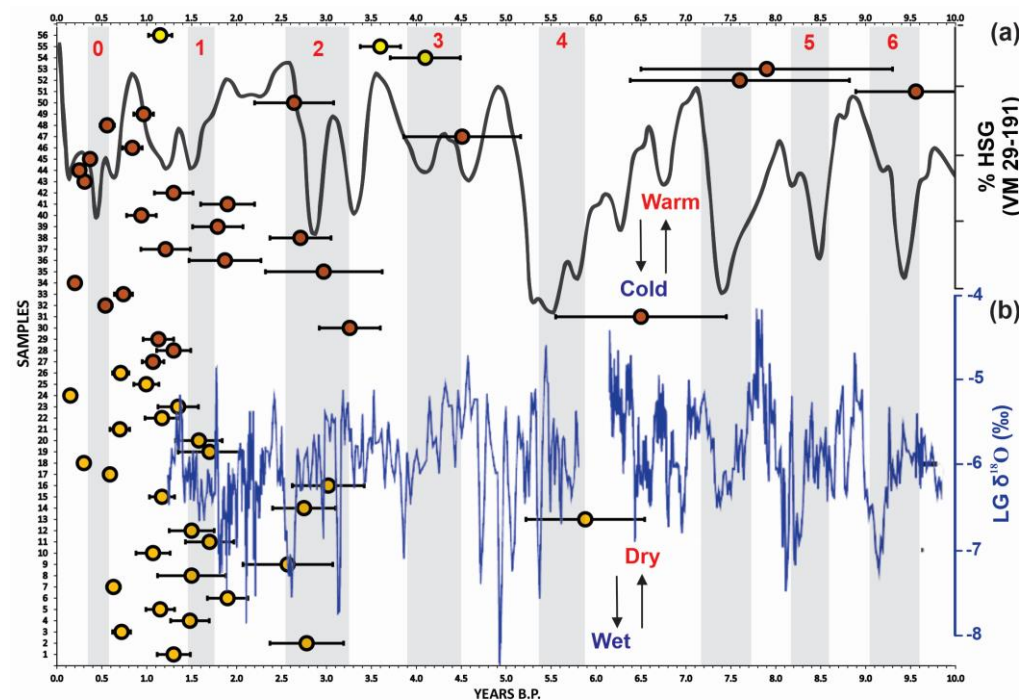


Figure 7. (a) Record of hematite-stained quartz grains (HSG) from the North Atlantic marine core VM 29-191 [15,56]. (b) Composite record of $\delta^{18}\text{O}$ from stalagmites LG3 and LG11, Lapa Grande cave, central east of Brazil [79]. Dots correspond to ages obtained by OSL dating for materials from low river terraces [27,34,37,68,70] (Supplementary Materials). Source: Adapted from Bond et al. [15,54], Strikis et al. [79], Cheng et al. [80], and Zielhofer et al. [81].

Additionally, when superimposed on the isotopic records of speleothems from the Lapa Grande cave located in the South Atlantic Convergence Zone (SACZ) corridor, most ages obtained for the depositional events present secular correlations linked to the periods

of rainfall intensification [79]. Rainfall events in the Early and Middle Holocene lasted ~ 300 years with amplitudes ranging from 0.9 ‰ to 1.5 ‰, while they were shorter in the Late Holocene, lasting ~ 100 years (Figure 7b) [79].

These paleoclimate dynamics developed different low terrace levels during the Holocene (See Figures 3 and 4). The oldest depositional ages (Early and Middle Holocene) correspond mostly to topographically higher single levels (N1) mainly correlated with Bond events 6, 5, and 4. Furthermore, the higher frequency of rains in shorter intervals of ~ 100 years explain the concentration of the depositional ages obtained in the Late Holocene, the elaboration of younger levels through recent erosive/depositional readjustments (Bond 0, 1, 2, and 3), and are responsible for developing terrace staircases composed of different levels (N1, N2, N3). In addition, in analyzing long-term variations between 10.0 and 1.0 ka (See Figure 7b), we observed an intensification of humid conditions for the period, which are determinant for the development of young low terraces closer to the current river channels [15,34,54,79–84].

Above all, such associations demonstrate that the continental geomorphological compartments of Southeastern Brazil, when compared to the others, showed greater sensitivity concerning the action of humid climate pulses throughout the Holocene (synchronous to Bond events), mainly in the Late Holocene, when events became shorter, abrupt, more frequent, and intense, resulting in the development of numerous levels of recent low river terraces. This recurrence possibly promoted more frequent adjustments in riverscapes through transitional phases, which explain the genesis of the channel incisions and the abandonment of old plains.

4.2. Southern Sertaneja Depression of Northeastern Brazil

Figure 8a shows a higher concentration of depositional ages outside of the periods associated with cooling pulses in the northern hemisphere, reinforcing the hypothesis of east-west dipole precipitation induced by the Walker circulation, persistent between the compartments located in the continental areas of Southeast and Northeast of Brazil [84]. This climate dipole also influenced the distribution of precipitation and temperature in Brazil during the Medieval Climate Anomaly, Little Ice Age, and the current modern warming period [21,60,83].

Dots correspond to ages obtained by OSL dating for materials from low river terraces (Supplementary Materials). Red dots represent ages obtained by OSL dating in the materials from low river terraces corresponding to the samples from the Southern Sertaneja Depression of Northeastern Brazil [69,72]. Horizontal bars indicate the standard deviation of dating. Vertical gray bars indicate Bond events from 0 to 6 [10,11,15,56], adapted from Stríkis et al. [79], Cheng et al. [80], and Zielhofer et al. [81].

However, isotopic records of speleothems from the Diva de Maura, Torrinha, and Lapa Doce caves (located in semi-arid climatic conditions) showed considerable secular correlations with the ages obtained for the surficial covers of low terraces (Figure 8b,c). These ages, when correlated with those from speleothems, indicate superimpositions with periods of intensified episodic rains, with the likely occurrence of depositions associated with Hortonian flows, typical of semi-arid environments [21,62].

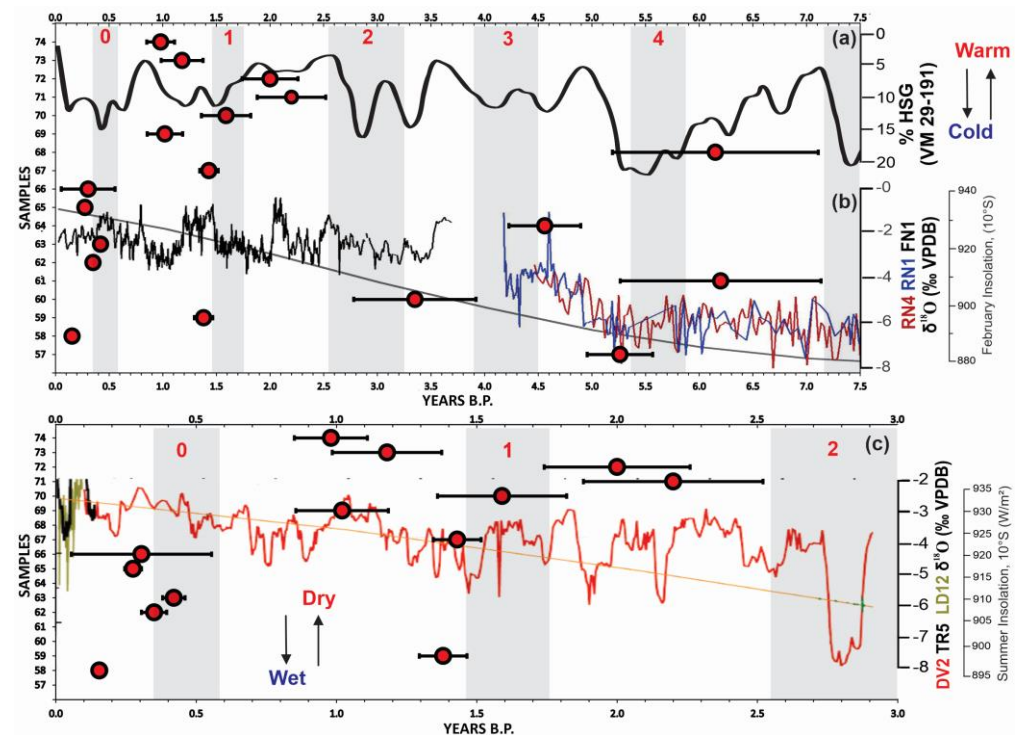


Figure 8. (a) Record of hematite-stained quartz grains (HSG) from the North Atlantic marine core VM 29–191 [15,54]. (b) Composite record of $\delta^{18}\text{O}$ from stalagmites RN4, RN1, and FN1, Rainha and Furna Nova caves, Northeastern Brazil [21], and February insolation at 10°S [84]. (c) Composite record of $\delta^{18}\text{O}$ from stalagmites DV2, TR5, and LD12, Diva de Maura, Torrinha, and Lapa Doce caves Northeastern Brazil, and February insolation at 10°S [62]. Dots correspond to ages obtained by OSL dating for materials from low river terraces [69,72] (Unpublished data in Supplementary Materials). Source: Adapted from Bond et al. [15,56], Cruz et al. [21], Zular et al. [84], Novello et al. [60], Strikis et al. [79], Cheng et al. [80], and Zielhofer et al. [81].

The long-term dry trend (4.2 to 0.0 ka) was interrupted by these sudden rainfall events, with periodicities of about 210 years (Figure 8b,c). The Bond 2 event, with an occurrence between about 2.8 and 2.65 ka, was the most intense period of humidity in the historical series of 3.0 ka [21,60]. This interpretation is based on the fact that most depositional ages of materials from low river terraces are correlated to events of intensification of relatively wetter and rainier periods in the semi-arid region, and which are represented by the drops in the lines of the isotopic records of speleothems from the Diva de Maura, Torrinha, and Lapa Doce caves (Figure 8c).

Considering the variance by geomorphological subcompartment and low terrace levels, older ages were also found, mainly for the inland subcompartments of the São Francisco Craton, with values of 5,234 ka (Figures 5 and 8b,c). When correlated with isotopic records of speleothems from the Rainha and Furna Nova caves (Figure 8b), the Middle Holocene ages (samples 57, 60, 61, 64, and 68) also indicate the deposition of materials from low river terraces during wetter episodes within the semi-arid context of Northeastern Brazil [21,84]. These episodes were likely linked to rainfall events of a greater magnitude which occurred in wetter conditions than the current ones throughout the Middle Holocene (7.5 to 4.2 ka), a period of remarkable variability of $\delta^{18}\text{O}$ on multidecadal to centenary timescales (Figure 8b).

4.3. Coastal Lowlands and Coastal Plains of the South, Southeast, and Northeast of Brazil

As depicted in Figure 9a, the geochronological results indicate that depositional events associated with the genesis of low river terraces in coastal compartments are not directly related to the influences exerted by the cooling pulses of the northern hemisphere [15,56],

as observed in the geomorphological compartments located in continental areas of the Northeast and Southeast of Brazil (climate dipole). However, the concentration of depositional ages in the Late Holocene—when correlated with isotopic records of the speleothems from the Botuverá (Figure 9b–d) and Cristal (Figure 9e) caves—is also associated with higher-intensity rainfall events along with the Holocene historical series [61,85–91].

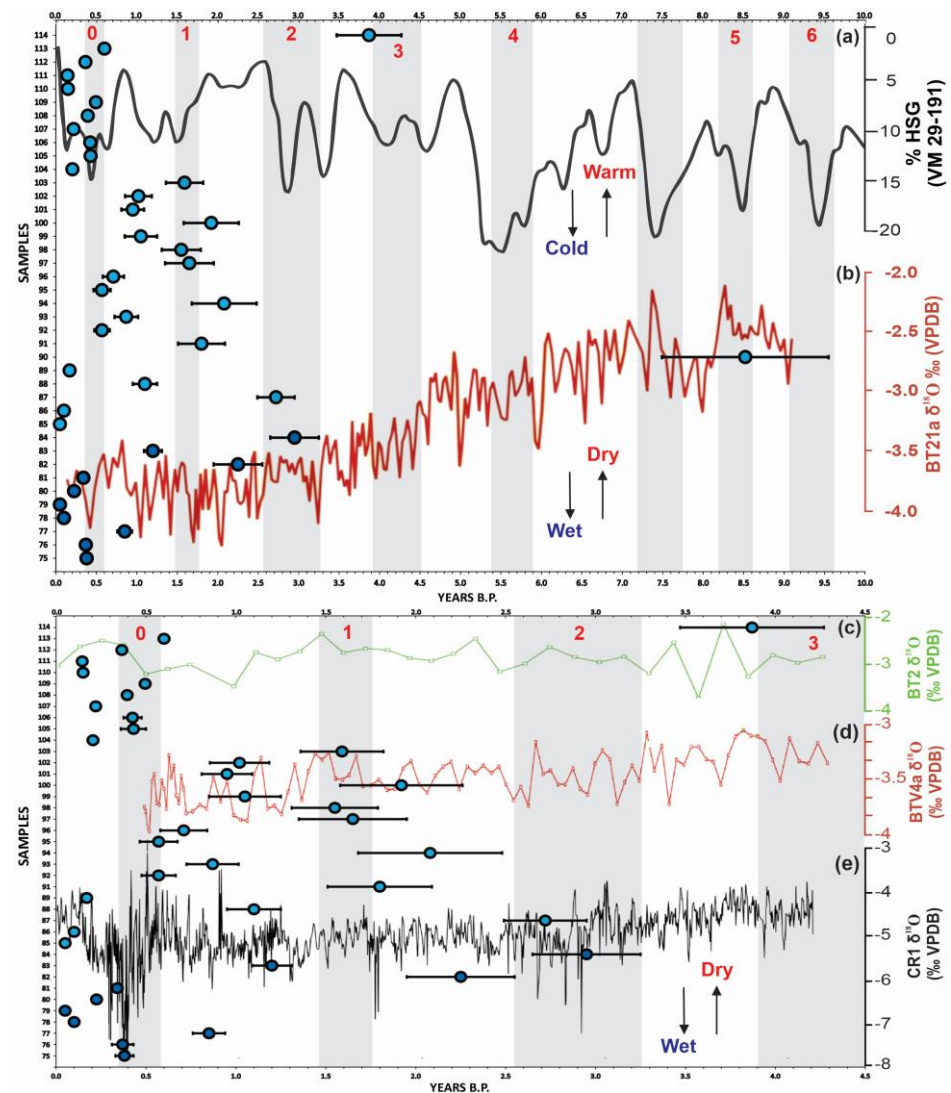


Figure 9. (a) Record of hematite-stained quartz grains (HSG) from the North Atlantic marine core VM 29–191 [15,54] (b) Composite record of $\delta^{18}O$ from stalagmite BT21a, Botuverá cave, Southern Brazil [86] (c) Composite record of $\delta^{18}O$ from stalagmite BT2, Botuverá cave, Southern Brazil [85]. (d) Composite record of $\delta^{18}O$ from stalagmite BTV4a, Botuverá cave, Southern Brazil [87]. (e) Composite record of $\delta^{18}O$ from stalagmite CR1, Cristal cave, Southeastern Brazil [88]. Dots correspond to ages obtained by OSL dating for materials from low river terraces [36,69,72,73,76] (Unpublished data in Supplementary Materials). Source: Adapted from Bond et al. [15,54], Bernal et al. [86], Cruz et al. [85], Wang et al. [87], Taylor [88], Strikis et al. [79], Cheng et al. [80], and Zielhofer et al. [81].

Such events are possibly intensified by the depositional processes which helped create low terraces in the Late Holocene, characterized by younger depositional ages than the continental samples. These interpretations corroborate the variations in the values of $\delta^{18}O$, with a downward trend in the last 9.0 ka (Figure 9b) and 4.0 ka (Figure 9d,e). Furthermore, due to the use of palynological proxies, there is a chronological superimposition with the periods which indicates the expansion of the Atlantic Forest in the coastal regions of

Southern Brazil; expansion of the Atlantic rainforest to the south of the Amazon rainforest along its southwest border; and the expansion of the moist Araucaria forest, replacing large pasture areas, mainly after 3.0 and 1.5/1.0 ka [59,83,89].

In this perspective, the rains, which correlated with the strengthening of SACZ observed in the Late Holocene, could supply the drainage headwaters of the Brazilian Atlantic Plateau, increasing volume, flow, transported sediment load, and flood pulses of rivers which flow into the Atlantic Ocean [89], thereby contributing to the deposition of materials in the low river terraces of the coastal plains.

Such trends, increasingly negative in values of $\delta^{18}\text{O}$, are the result of an increase in summer solar radiation, SAMS intensity, and south migration of the SACZ average position through the recovery and increase in moisture from the Amazon basin to the Southeast and South of Brazil until modern conditions were reached [61,85–88]. However, the climate dynamics relating to paleo-precipitation are also influenced by other atmospheric circulation activities in the tropical and subtropical Atlantic regions, such as the South Atlantic Subtropical High (SASH) and the polar cold fronts, which affect the Atlantic climate in both summer and winter [82,83].

The driest period is linked to the medieval climate anomaly (~1.12–0.92) (Figure 9e), caused by the weakening of the monsoon system and the decrease in summer precipitation, and the wettest period of the historical series is associated with the Little Ice Age (~0.42–0.2) (Figure 9e) [59,88]. Climate pulses are essential in understanding the development of Holocene low river terraces located in the coastal plains of Brazil.

5. Conclusions

The concentration of Holocene depositional ages in the compartments analyzed in the present study was associated with rainfall events of greater intensities, but with rhythms and intensities that varied over time due to different responses induced by the specificities of each environmental system. In this perspective, the global climate zones were not responsible for forming low river terraces, but events relating to local/regional climate pulses which guided the remobilization of sediments and the abandonment of old plains by fluvial incisions.

Statistical analyses revealed a greater correlation between latitude/longitude variables and compartments and subcompartments, to the detriment of the other variables. These analyses showed different responses of environmental systems to the action of Holocene climate pulses, with morphogenetic distinctions between inland and coastal groups as well as inland subgroups.

The results also contribute to a better understanding of river dynamics at different scales, expanding discussions on the relationship between low river terraces as responses to Holocene climatic pulses, comprising forms developed during periods of hydrological instabilities.

In the Paulista Peripheral Depression, Paulista Western Plateau, and Central Plateau, the deposition of materials from low river terraces in Southeastern Brazil occurred most often during rainy episodes, coinciding with Bond events.

In the Southern Sertaneja Depression of Northeastern Brazil, most depositional events were located outside the periods associated with the cooling pulses in the northern hemisphere, enhancing the hypothesis of an enduring east-west precipitation dipole between the compartments located in the continental sectors of the Southeast and Northeast of Brazil.

In the coastal lowlands and coastal plains of the South, Southeast, and Northeast of Brazil, the depositional events failed to present a direct relationship with the influences exerted by the cooling pulses of the northern hemisphere. However, the concentration of the depositional ages in the Late Holocene is also associated with higher intensity rainfall events, along with the Holocene historical series.

Supplementary Materials: The following supporting information can be downloaded at: <https://www.mdpi.com/article/10.3390/w14192977/s1>, Location and environmental conditions of the supplementary data of 114 absolute dating obtained from Optically Stimulated Luminescence (OSL) on surficial covers associated with low river.

Author Contributions: Project Administration and Funding Acquisition, A.P.F.; Software and Validation, A.F.M. and C.Z.; Data Curation, V.B.M. and L.L.; Discussion and Writing—original draft Preparation, A.O.S., B.A.T., M.M.P., F.G.R., D.O.B.F.M., É.V.V., P.I.C.A., L.L. and V.B.M.; Writing—review and editing, A.F.M., C.Z., A.O.S., B.A.T., M.M.P., F.G.R., D.O.B.F.M., É.V.V., P.I.C.A., L.L. and V.B.M. All authors have read and agreed to the published version of the manuscript.

Funding: This research was funded by São Paulo Research Foundation (FAPESP), grants 2011/21491-7, 2012/00145-6, 2013/24885-1, 2014/03894-5, 2015/10417-1, 2016/24390-0, 2016/00382-9, 2016/21335-9, 2016/08944-6, 2016/05327-6, 2017/26876-0, 2018/23828-8, 2018/07271-3, 2019/23452-0, 2020/15004-5, 2021/05823-1, and National Council for Scientific and Technological Development (CNPq), grant 304751/2020-0.

Institutional Review Board Statement: Not applicable.

Informed Consent Statement: Informed consent was obtained from all subjects involved in the study.

Data Availability Statement: The data presented in this study are available on request from the corresponding author.

Conflicts of Interest: The authors declare no conflict of interest.

References

1. Brunnsden, D.; Thornes, J.B. Landscape sensitivity and change. *Trans. Inst. Br. Geogr.* **1979**, *4*, 463–484. [\[CrossRef\]](#)
2. Errico, A.; Lama, G.F.C.; Francalanci, S.; Chirico, G.B.; Solari, L.; Preti, F. Flow dynamics and turbulence patterns in a drainage channel colonized by common reed (*Phragmites australis*) under different scenarios of vegetation management. *Ecol. Eng.* **2019**, *133*, 39–52. [\[CrossRef\]](#)
3. Lama, G.F.C.; Rillo Migliorini Giovannini, M.; Errico, A.; Mirzaei, S.; Padulano, R.; Chirico, G.B.; Preti, F. Hydraulic Efficiency of Green-Blue Flood Control Scenarios for Vegetated Rivers: 1D and 2D Unsteady Simulations. *Water* **2021**, *13*, 2620. [\[CrossRef\]](#)
4. Phillips, J.D. Sources of nonlinearity and complexity in geomorphic systems. *Prog. Phys. Geogr.* **2003**, *27*, 1–23. [\[CrossRef\]](#)
5. Phillips, J.D. Emergence and pseudo-equilibrium in geomorphology. *Geomorphology* **2011**, *132*, 319–326. [\[CrossRef\]](#)
6. Benito, G.; Machado, M.J.; Pérez-González, A. Climate change and flood sensitivity in Spain. *Geol. Soc. Lond. Spec. Publ.* **1996**, *115*, 85–98. [\[CrossRef\]](#)
7. Boer, D.H. Hierarchies and spatial scale in process geomorphology: A review. *Geomorphology* **1992**, *4*, 303–318. [\[CrossRef\]](#)
8. Fryirs, K. (Dis) Connectivity in catchment sediment cascades: A fresh look at the sediment delivery problem. *Earth Surf. Process. Landf.* **2012**, *38*, 30–46. [\[CrossRef\]](#)
9. Fryirs, K.A. River sensitivity: A lost foundation concept in fluvial geomorphology. *Earth Surf. Process. Landf.* **2017**, *42*, 55–70. [\[CrossRef\]](#)
10. Lama, G.F.C.; Crimaldi, M.; Pasquino, V.; Padulano, R.; Chirico, G.B. Bulk Drag Predictions of Riparian *Arundo donax* Stands through UAV-acquired Multispectral Images. *Water* **2021**, *13*, 1333. [\[CrossRef\]](#)
11. Lama, G.F.C.; Errico, A.; Francalanci, S.; Solari, L.; Preti, F.; Chirico, G.B. Evaluation of Flow Resistance Models Based on Field Experiments in a Partly Vegetated Reclamation Channel. *Geosciences* **2020**, *10*, 47. [\[CrossRef\]](#)
12. Wohl, E.; Brierley, G.; Cadol, D.; Coulthard, T.J.; Covino, T.; Fryirs, K.A.; Grant, G.; Hilton, R.G.; Lane, S.N.; Magilligan, F.J.; et al. Connectivity as an emergent property of geomorphic systems. *Earth Surf. Process. Landf.* **2019**, *44*, 4–26. [\[CrossRef\]](#)
13. Schumm, S.A. Geomorphic thresholds: The concept and its applications. *Trans. Inst. Br. Geogr.* **1979**, *4*, 485–515. [\[CrossRef\]](#)
14. Schumm, S.A.; Lichty, R.W. Time, space, and causality in geomorphology. *Am. J. Sci.* **1965**, *263*, 110–119. [\[CrossRef\]](#)
15. Bond, G.; Kromer, B.; Beer, L.; Muscheler, R.; Evans, M.N.; Showers, W.; Hoffmann, S.; Lotti-Bond, R.; Hajdas, I.; Bonani, G. Persistent solar influence on North Atlantic climate during the Holocene. *Science* **2001**, *294*, 2130–2136. [\[CrossRef\]](#)
16. Bradley, R.S.; Hughes, M.K.; Diaz, H.F. Climate in medieval time. *Science* **2003**, *302*, 404–405. [\[CrossRef\]](#)
17. Vandenberghe, J. Timescales, climate and river development. *Quat. Sci. Rev.* **1995**, *14*, 631–638. [\[CrossRef\]](#)
18. Vandenberghe, J. Climate forcing of fluvial system development: An evolution of ideas. *Quat. Sci. Rev.* **2003**, *22*, 2053–2060. [\[CrossRef\]](#)
19. Thomas, M.F. Landscape sensitivity in time and space—An introduction. *Catena* **2001**, *42*, 83–98. [\[CrossRef\]](#)
20. Breda, C.; Pupim, F.N.; Sawakuchi, A.O.; Mineli, T.D. The role of bedrock and climate for the late Quaternary erosive-depositional behavior of an intraplate tropical river: The Tietê River case, southeastern Brazil. *Geomorphology* **2021**, *389*, 107834. [\[CrossRef\]](#)
21. Cruz, F.W.; Vuille, M.; Burns, S.J.; Wang, X.; Cheng, H.; Werner, M.; Edwards, R.L.; Karmann, I.; Auler, A.S.; Nguyen, H. Orbitally driven east-west antiphasing of South American precipitation. *Nat. Geosci.* **2009**, *2*, 210–214. [\[CrossRef\]](#)

22. Butzer, K.W. Holocene alluvial sequences: Problems of dating and correlation. *Timescales Geomorphol.* **1980**, 131–142.
23. Taylor, M.P.; Macklin, M.G.; Hudson-Edwards, K. River sedimentation and fluvial response to Holocene environmental change in the Yorkshire Ouse Basin, northern England. *Holocene* **2000**, *10*, 201–212. [[CrossRef](#)]
24. Macklin, M.G.; Lewin, J. River sediments, great floods and centennial-scale Holocene climate change. *J. Quat. Sci.* **2003**, *18*, 101–105. [[CrossRef](#)]
25. Macklin, M.G.; Jones, A.F.; Lewin, J. River response to rapid Holocene environmental change: Evidence and explanation in British catchments. *Quat. Sci. Rev.* **2010**, *29*, 1555–1576. [[CrossRef](#)]
26. Macklin, M.G.; Lewin, J.; Jones, A.F. River entrenchment and terrace formation in the UK Holocene. *Quat. Sci. Rev.* **2013**, *76*, 194–206. [[CrossRef](#)]
27. Dias, R.L. Geocronologia Da Cobertura Superficial Em Níveis Geomorfológicos Do Setor Centro-Ocidental Na Depressão Periférica Paulista. Ph.D. Thesis, Universidade Estadual de Campinas, São Paulo, Brazil, 2015.
28. Haug, G.H.; Hughen, K.A.; Sigman, D.M.; Peterson, L.C.; Röhl, U. Southward migration of the intertropical convergence zone through the Holocene. *Science* **2001**, *293*, 1304–1308. [[CrossRef](#)]
29. Latrubesse, E.M.; Stevaux, J.C.; Sinha, R. Tropical rivers. *Geomorphology* **2005**, *70*, 187–206. [[CrossRef](#)]
30. Sinha, R.; Jain, V.; Babu, G.P.; Ghosh, S. Geomorphic characterization and diversity of the fluvial systems of the Gangetic Plains. *Geomorphology* **2005**, *70*, 207–225. [[CrossRef](#)]
31. Leli, I.T.; Stevaux, J.C.; Assine, M.L. Origin, evolution, and sedimentary records of islands in large anabranching tropical rivers: The case of the Upper Paraná River, Brazil. *Geomorphology* **2020**, *358*, 107118. [[CrossRef](#)]
32. Khan, M.A.; Sharma, N.; Lama, G.F.C.; Hasan, M.; Garg, R.; Busico, G.; Alharbi, R.S. Three-Dimensional Hole Size (3DHS) Approach for Water Flow Turbulence Analysis over Emerging Sand Bars: Flume-Scale Experiments. *Water* **2022**, *14*, 1889. [[CrossRef](#)]
33. Dias, R.L.; Perez Filho, A. Geocronologia de terraços fluviais na bacia hidrográfica do rio Corumbataí-SP a partir de Luminescência Opticamente Estimulada (LOE). *Rev. Bras. Geomorfol.* **2015**, *16*, 341–349. [[CrossRef](#)]
34. Storani, D.L. Cenário Regional das Oscilações Climáticas Quaternárias: Baixos Terraços Fluviais no Contexto da Depressão Periférica e do Planalto Ocidental Paulista. Ph.D. Thesis, Universidade Estadual de Campinas, São Paulo, Brazil, 2015; 104p.
35. Valezio, E.V.; Perez Filho, A. Dinâmica antrópica no canal fluvial do córrego Tucum–São Pedro, São Paulo (Brasil). *Rev. Bras. Geomorfol.* **2016**, *16*, 545–557. [[CrossRef](#)]
36. Rubira, F.G.; Perez Filho, A. Geochronology and hydrodynamic energy conditions in surface coverings of low Holocene fluvial, fluvialmarine, and marine terraces: Climatic pulsations to the south of the Aranguaguá River Basin (SC). *Rev. Bras. Geomorfol.* **2018**, *19*, 635–663. [[CrossRef](#)]
37. Souza, A.O.; Perez Filho, A. Processos, ambientes deposicionais e geocronológicas das coberturas superficiais sobre aplainamentos neogênicos e terraços fluviais na bacia do Ribeirão Araquá, Depressão Periférica Paulista. *Rev. Bras. Geomorfol.* **2018**, *19*, 107–126. [[CrossRef](#)]
38. Souza, A.O.; Perez Filho, A. Late Holocene coastal dynamics, climate pulses and low terraces in the coast of the state of São Paulo, southeast, Brazil. *J. S. Am. Earth Sci.* **2019**, *92*, 234–245. [[CrossRef](#)]
39. Perez Filho, A.; Rubira, F.G. Evolutionary interpretation of Holocene landscapes in eastern Brazil by optimally stimulated luminescence: Surface coverings and climatic pulsations. *Catena* **2019**, *172*, 866–876. [[CrossRef](#)]
40. Moreira, V.B.; Perez Filho, A. Geocronologia da cobertura superficial em baixos terraços fluviais na chapada Uberlândia-Uberaba/MG. *Rede Rev. Eletrônica Prodema* **2019**, *13*, 89–100. [[CrossRef](#)]
41. Rasbold, G.G.; Mcglue, M.M.; Stevaux, J.C.; Parolin, M.; Silva, A.; Bergier, I. Sponge spicule and phytolith evidence for Late Quaternary environmental changes in the tropical Pantanal wetlands of western Brazil. *Palaeogeogr. Palaeoclimatol. Palaeoecol.* **2019**, *518*, 119–133. [[CrossRef](#)]
42. Lima, K.C.; Perez Filho, A.; Lupinacci, C.M.; Valezio, E.V.; Góes, L.M. Fluvial responses to external and internal forcing: Upper Holocene dynamics in a low latitude semi-arid region in South America. *J. S. Am. Earth Sci.* **2021**, *112*, 103545. [[CrossRef](#)]
43. Souza, A.O.; Lämmle, L.; Perez Filho, A.; Donadio, C. Recent geomorphological changes in the Paraíba do Sul delta, South America East Coast. *Prog. Phys. Geogr.* **2022**, *46*, 566–588. [[CrossRef](#)]
44. Lämmle, L.; Perez Filho, A.; Donadio, C.; Moreira, V.B.; Santos, C.J.; Souza, A.O. Baixos terraços marinhos associados às transgressões e regressões marinhas holocênicas na Planície Costeira do rio Paraíba do Sul, Rio de Janeiro, Brasil. *Rev. Bras. Geomorfol.* **2022**, *23*, 1285–1303. [[CrossRef](#)]
45. Wanner, H.; Solomina, O.; Grosjean, M.; Ritz, S.P.; Jetel, M. Structure and origin of Holocene cold events. *Quat. Sci. Rev.* **2011**, *30*, 3109–3123. [[CrossRef](#)]
46. Kennett, D.J.; Breitenbach, S.F.; Aquino, V.V.; Asmeron, Y.; Awe, J.; Baldini, J.U.L.; Bartlein, P.; Culleton, B.J.; Ebert, C.; Jazwa, C.; et al. Development and disintegration of Maya political systems in response to climate change. *Science* **2012**, *338*, 788–791. [[CrossRef](#)] [[PubMed](#)]
47. Walker, M.; Head, M.J.; Berkelhammer, M.; Björck, S.; Cheng, H.; Cwynar, L.; Fisher, D.; Gkinis, V.; Long, A.; Lowe, J.; et al. Formal ratification of the subdivision of the Holocene Series/Epoch (Quaternary System/Period): Two new Global Boundary Stratotype Sections and Points (GSSPs) and three new stages/subseries. *Episodes* **2018**, *41*, 213–223. [[CrossRef](#)]
48. Koch, A.; Brierley, C.; Maslin, M.M.; Lewis, S.L. Earth system impacts of the European arrival and Great Dying in the Americas after 1492. *Quat. Sci. Rev.* **2019**, *207*, 13–36. [[CrossRef](#)]

49. Leopold, L.B.; Wolman, M.G.; Miller, J.P. *Fluvial Processes in Geomorphology*; W. H. Freeman and Company: San Francisco, CA, USA, 1964.
50. Moy, C.M.; Seltzer, G.O.; Rodbell, D.T.; Anderson, D.M. Variability of El niño/ southern oscillation activity at millennial timescales during the Holocene epoch. *Nature* **2002**, *420*, 162. [[CrossRef](#)] [[PubMed](#)]
51. Moreira, V.B.; Perez Filho, A. Das superfícies de aplainamento aos pulsos climáticos holocênicos: A evolução da paisagem em relevos de chapada. *Soc. Nat.* **2020**, *32*, 176–195. [[CrossRef](#)]
52. Souza, A.O.; Perez Filho, A.; Lämmle, L.; Souza, D.H. Holocene climate pulses and structural controls on the geomorphological estuarine evolution of The Iguape River, São Paulo, Brazil. *Cont. Shelf Res.* **2020**, *205*, 104168. [[CrossRef](#)]
53. Ljungqvist, F.C. A new reconstruction of temperature variability in the extra-tropical Northern Hemisphere during the last two millennia. *Geogr. Ann. Ser. A Phys. Geogr.* **2010**, *92*, 339–351. [[CrossRef](#)]
54. Bond, G.; Showers, W.; Cheseby, M.; Lotti, R.; Almasi, P.; Menocal, P.; Priore, P.; Cullen, H.; Hajdas, I.; Bonani, G. A pervasive millennial-scale cycle in the North Atlantic Holocene and glacial climates. *Science* **1997**, *278*, 1257–1266. [[CrossRef](#)]
55. Bahr, A.; Kaboth-Bahr, S.; Jaeschke, A.; Chiessi, C.; Cruz, F.; Carvalho, L.; Rethemeyer, J.; Schefuß, E.; Geppert, P.; Alburquerque, A.L.; et al. Late Holocene Precipitation Fluctuations in South America Triggered by Variability of the North Atlantic Overturning Circulation. *Paleoceanogr. Paleoclimatol.* **2021**, *36*, e2021PA004223. [[CrossRef](#)]
56. Behling, H. Late Quaternary vegetational and climatic changes in Brazil. *Rev. Palaeobot. Palynol.* **1998**, *99*, 143–156. [[CrossRef](#)]
57. Behling, H. South and southeast Brazilian grasslands during Late Quaternary times: A synthesis. *Palaeogeogr. Palaeoclimatol. Palaeoecol.* **2002**, *77*, 19–27. [[CrossRef](#)]
58. Pessenda, L.C.R.; Saia, S.E.M.G.; Gouveia, S.E.M.; Ledru, M.P.; Sifeddine, A.; Amaral, P.G.C.; Bendassolli, J.A. Last millennium environmental changes and climate inferences in the Southeastern Atlantic forest, Brazil. *An. Acad. Bras. Ciências* **2010**, *82*, 717–729. [[CrossRef](#)]
59. Vuille, M.; Burns, S.J.; Taylor, B.L.; Cruz, F.W.; Bird, B.W.; Abbott, M.B.; Kanner, L.C.; Cheng, H.; Novello, V.F. A review of the South American monsoon history as recorded in stable isotopic proxies over the past two millennia. *Clim. Past* **2012**, *8*, 1309–1321. [[CrossRef](#)]
60. Novello, V.F.; Cruz, F.W.; Karmann, I.; Burns, S.J.; Stríkis, N.M.; Vuille, M.; Cheng, H.; Edwards, R.L.; Santos, R.V.; Frigo, E.; et al. Multidecadal climate variability in Brazil's Nordeste during the last 3000 years based on speleothem isotope records. *Geophys. Res. Lett.* **2012**, *39*, 1–6. [[CrossRef](#)]
61. Pazzaglia, F.J. Fluvial Terraces. In *Treatise on Geomorphology*; Academic Press: Cambridge, MA, USA, 2013; Volume 9, pp. 379–412.
62. Vandenberghe, J. River terraces as a response to climatic forcing: Formation processes, sedimentary characteristics and sites for human occupation. *Quat. Int.* **2015**, *370*, 3–11. [[CrossRef](#)]
63. Perez Filho, A.; Donezelli, J.L.; Lepsch, I.F. Relação Solos Geomorfologia em Várzea Do Rio Moji-Guaçu (SP). *Rev. Bras. Ciência Solo* **1980**, *4*, 181–187.
64. de Mello Araujo, A.G.; Feathers, J.K.; Hartmann, G.A.; Ladeira, F.S.; Valezio, É.V.; Nascimento, D.L.; Ricci, O.; Marum, V.J.O.; da Trindade, R.I.F. Revisiting Alice Boer: Site formation processes and dating issues of a supposedly pre-Clovis site in Southeastern Brazil. *Geoarchaeology* **2020**, *37*, 32–58. [[CrossRef](#)]
65. Lu, H.; Zhang, H.; Wang, S.J.; Cosgrove, R.; Sun, X.; Zhao, J.; Sun, D.; Zhao, C.; Shen, C.; Wei, M. Multiphase timing of hominin occupations and the paleoenvironment in Luonan Basin, Central China. *Quat. Res.* **2011**, *76*, 142–147. [[CrossRef](#)]
66. Panin, A.V.; Nefedov, V.S. Analysis of variations in the regime of river and lakes in the Upper Volga and Upper Zapadnaya Dvina based on archaeological-geomorphological data. *Water Resour.* **2010**, *37*, 16–32. [[CrossRef](#)]
67. Silva, V.A. Geomorfologia Antropogênica: Mudanças no Padrão de Drenagem do Canal Principal e Delta, no Baixo Curso da Bacia Hidrográfica do Rio Jequitinhonha/BA. 186p. Ph.D. Thesis, Universidade Estadual de Campinas, São Paulo, Brazil, 2012.
68. Valezio, E.V. Equilíbrio em Geomorfologia: Geossistemas, Planícies de Inundação e Morfodinâmica dos Rios Jacaré-Pepira e Jacaré-Guaçu (SP). Master's Thesis, Universidade Estadual de Campinas, São Paulo, Brazil, 2016; 110p.
69. Lima, K.C. O Holoceno Superior na Bacia do rio Itapicuru (Bahia/Brasil): Proposição de Cenário Para o Baixo Curso e Planície Costeira. Ph.D. Thesis, Universidade Estadual de Campinas, São Paulo, Brazil, 2017.
70. Moreira, V.B. Geocronologia em Ambientes de Veredas e Campos de Murundus na Chapada Uberlândia-Uberaba: Subsídios à Evolução da Paisagem. Master's Thesis, Universidade Estadual de Campinas, São Paulo, Brazil, 2017.
71. Rodrigues, G.B. Geocronologia das Coberturas Superficiais em Baixos Terraços e na Foz da Bacia Hidrográfica do Rio Jequitinhonha (BA) Relacionada Com as Oscilações Climáticas do Holoceno. Master's Thesis, Universidade Estadual de Campinas, São Paulo, Brazil, 2018.
72. Goes, L.M. Geocronologia das Coberturas Superficiais nos Baixos Terraços Fluviais e Aluviões Recentes no Médio Curso da Bacia Hidrográfica do Rio Itapicuru (Bahia-Brasil). Ph.D. Thesis, Universidade Estadual de Campinas, São Paulo, Brazil, 2019.
73. Rubira, F.G. Espacialização e Geocronologia das Coberturas Superficiais em Baixos Terraços Marinhos, Fluviomarinhas e Fluviais na foz das Bacias dos Rios Itapocu e Araranguá (SC), Decorrentes dos Episódios Eustáticos Associados às Oscilações climáticas. Ph.D. Thesis, Universidade Estadual de Campinas, São Paulo, Brazil, 2019.
74. Moreira, V.B. Geocronologia de Coberturas Superficiais em Baixos Terraços na Foz dos Rios Una/Pardo (BA), Relacionados a Transgressões e Regressões Marinhas Decorrentes de Pulsões Climáticas Holocênicas. Ph.D. Thesis, Universidade Estadual de Campinas, São Paulo, Brazil, 2021.

75. Souza, A.O. Geocronologia das Coberturas Superficiais em Baixos Terraços Fluviais, Marinheiros e Fluvio-Marinheiros na Foz das Bacias do Ribeira de Iguape-SP e do Rio Paraíba do Sul-RJ: Flutuações Climáticas Holocênicas no Sudeste Brasileiro. Ph.D. Thesis, Universidade Estadual de Campinas, São Paulo, Brazil, 2019.
76. Rubira, F.G.; Perez Filho, A. Geocronologia De Eventos Deposicionais Associados Às Coberturas Superficiais Que Sustentam E Recobrem Níveis De Terraços Marinheiros Pleistocênicos E Holocênicos No Litoral Sul De Santa Catarina (SC). *Rev. Bras. Geomorfol.* **2019**, *20*, 581–602. [[CrossRef](#)]
77. Wintle, A.G.; Murray, A.S. A review of quartz optically stimulated luminescence characteristics and their relevance in single-aliquot regeneration dating protocols. *Rations Meas.* **2006**, *41*, 369–391. [[CrossRef](#)]
78. Murray, A.S.; Mejdahl, V. Comparison of regenerative dose single-aliquot and multiple-aliquot protocols using heated quartz from archaeological sites. *Quat. Sci. Rev.* **1999**, *18*, 223–229. [[CrossRef](#)]
79. Strikis, N.M.; Cruz, F.W.; Cheng, H.; Karmann, I.; Edwards, R.L.; Vuille, M.; Wang, X.; Paula, M.S.; Novello, V.F.; Auler, A.S. Abrupt variations in South American monsoon rainfall during the Holocene based on a speleothem record from central-eastern Brazil. *Geology* **2011**, *39*, 1075–1078. [[CrossRef](#)]
80. Cheng, H.; Sinha, A.; Wang, X.; Cruz, F.W.; Edwards, R.L. The Global Paleomonsoon as seen through speleothem records from Asia and the Americas. *Clim. Dyn.* **2012**, *39*, 1045–1062. [[CrossRef](#)]
81. Zielhofer, C.; Köhler, A.; Mischke, S.; Benkaddour, A.; Mikdad, A.; Fletcher, W.J. Western Mediterranean hydro-climatic consequences of Holocene ice-rafted debris (Bond) events. *Clim. Past* **2019**, *15*, 463–475. [[CrossRef](#)]
82. Rubira, F.G.; Perez Filho, A. Evolução das bases teóricas e metodológicas para identificação das mudanças, oscilações e pulsações climáticas. *Rev. Bras. Geomorfol.* **2021**, *22*, 922–966. [[CrossRef](#)]
83. Smith, R.J.; Mayle, F.E. Impact of mid- to late Holocene precipitation changes on vegetation across lowland tropical South America: A paleo-data synthesis. *Quat. Res.* **2018**, *89*, 134–155. [[CrossRef](#)]
84. Zular, A.; Utida, G.; Cruz, F.W.; Sawakuchi, A.O.; Wang, H.; Bicego, M.; Giannini, P.C.F.; Rodrigues, S.I.; Garcia, G.P.B.; Vuille, M.; et al. The effects of mid-Holocene fluvio-eolian interplay and coastal dynamics on the formation of dune-dammed lakes in NE Brazil. *Quat. Sci. Rev.* **2018**, *196*, 137–153. [[CrossRef](#)]
85. Cruz, F.W.; Burns, S.J.; Karmann, I.; Sharp, W.D.; Vuille, M.; Cardoso, A.O.; Ferrari, J.A.; Dias, P.L.S.; Viana Júnior, O. Insolation-driven changes in atmospheric circulation over the past 116,000 years in subtropical Brazil. *Nature* **2005**, *434*, 63–66. [[CrossRef](#)]
86. Bernal, J.P.; Cruz, F.W.; Strikis, N.M.; Wang, X.; Deininger, M.M.; Catunda, M.C.A.; Ortega-Obregón, C.; Cheng, H.; Edwards, R.L.; Auler, A.S. High-resolution Holocene South American monsoon history recorded by a speleothem from Botuverá Cave, Brazil. *Earth Planet. Sci. Lett.* **2016**, *450*, 186–196. [[CrossRef](#)]
87. Wang, X.; Auler, A.S.; Edwards, R.L.; Cheng, H.; Ito, E.; Solheid, M. Interhemispheric anti-phasing of rainfall during the last glacial period. *Quat. Sci. Rev.* **2006**, *25*, 3391–3403. [[CrossRef](#)]
88. Taylor, B.L. A Speleothems-Based Highresolution Reconstruction of Climate in Southeastern Brazil over the Past 4,100 years. 97f. Ph.D. Thesis, Department of Geosciences, University of Massachusetts Amherst, Amherst, MA, USA, 2010.
89. Rodrigues, J.M.; Behling, H.; Giesecke, T. Holocene dynamics of vegetation change in southern and southeastern Brazil is consistent with climate forcing. *Quat. Sci. Rev.* **2016**, *146*, 54–65. [[CrossRef](#)]
90. Busico, G.; Buffardi, C.; Ntona, M.M.; Vigliotti, M.; Colombani, N.; Mastrocicco, M.; Ruberti, D. Actual and Forecasted Vulnerability Assessment to Seawater Intrusion via GALDIT-SUSI in the Volturno River Mouth (Italy). *Remote Sens.* **2021**, *13*, 3632. [[CrossRef](#)]
91. Freedman, D.; Pisani, R.; Purves, R. *Statistics: Fourth International Student Edition 2021*; W. W. Norton & Company: New York, NY, USA, 2021; Available online: <https://www.amazon.com/Statistics-Fourth-International-Student-Freedman/dp/0393930432> (accessed on 18 September 2022).